







Cite this: *RSC Adv.*, 2025, 15, 45427

# MgAl and ZnAl layered double hydroxides as efficient sorbents for phosphorus recovery from water

Inês D. Borges, <sup>\*abc</sup> Cláudia M. Rocha, <sup>b</sup> Frederico Maia, <sup>b</sup> Carlos M. Silva <sup>ac</sup> and Margarida J. Quina <sup>\*a</sup>

The global scarcity of phosphorus and increasing concern over aquatic eutrophication are driving greater interest in phosphorus (P) recovery from water. Emerging materials, such as Layered Double Hydroxides (LDH) or their calcined forms, Layered Double Oxides (LDO), are gaining attention for their excellent sorption capacity. This study aims to evaluate the performance of three different materials, a calcined MgAl-LDO, ZnAlNO<sub>3</sub>, and its calcined product ZnAl-LDO for phosphate removal in batch conditions. The foremost strength of this article is that the materials under studied are manufactured on a large scale, thereby facilitating the scaling up for practical applications. The materials were characterized by X-ray diffraction (XRD) and Fourier transform infrared (FTIR) before and after sorption. After calcination, MgAl-LDO reacquires its initial structure when in contact with an aqueous solution due to the "memory effect", whereas ZnAl-LDO maintains its metal oxide state. Phosphorus removal by both calcined and non-calcined materials followed a pseudo-second-order kinetics. The ZnAlNO<sub>3</sub> revealed a higher removal capacity when compared to ZnAl-LDO, which indicates that, in this case, the calcination does not improve its sorption capacity. The equilibrium study using ZnAlNO<sub>3</sub> demonstrated that the Langmuir isotherm provided the best fit for the experimental data, with a maximum phosphorus loading capacity of 84 mg g<sup>-1</sup>. Overall, ZnAlNO<sub>3</sub> appears to be a promising sorbent for the efficient and cost-effective removal of phosphate ions from eutrophicated water streams.

Received 29th July 2025  
Accepted 27th October 2025

DOI: 10.1039/d5ra05491e

rsc.li/rsc-advances

## 1. Introduction

Elemental phosphorus, known for 350 years, is one of the essential chemical elements for life on Earth, and is considered a non-renewable and irreplaceable resource, with a critical role in agriculture production.<sup>1–3</sup> Phosphorus is essential for all living organisms, playing a key role in the formation of DNA and RNA (as orthophosphate, PO<sub>4</sub><sup>3–</sup>), energy transfer through ATP in living cells, and the formation of cell membranes *via* phospholipids.<sup>1,4</sup> Following the trend of world population growth, P demand for agriculture (food production and biofuels) has increased significantly. It is estimated that in the middle of this century, the world population will exceed nine billion, which means that food production will have to increase by almost 30%.<sup>5</sup> Approximately 65% of global phosphorus has been mined in a few countries, including China, Morocco, and USA.<sup>6</sup> Phosphate rock and phosphorus are both classified as critical raw materials (CRM) for the European Union (EU), which

heavily depends on imports. Currently, P is mainly obtained from mining phosphate rock, and the manufacturing of mineral fertilizers is the main application. In the phosphorus cycle, a critical concern is related to the inefficiencies and losses associated with phosphate fertilizer production/utilization, which leads to the accumulation of P in water bodies, causing eutrophication. Indeed, phosphorus concentrations above 2 mg L<sup>-1</sup> can accelerate significantly eutrophication phenomena.<sup>1</sup> The global phosphorus situation presents a complex challenge: on one hand, excess phosphorus in water bodies leads to eutrophication and impaired water quality. On the other hand, there are concerns about the potential future scarcity of phosphorus for agricultural production due to the finite nature of phosphate rock reserves. This dual issue of local excess and potential future scarcity highlights the need for improved phosphorus management and resource efficiency, with the recovery of P from wastewater as a valuable strategy.<sup>7–9</sup>

Layered Double Hydroxides (LDH) are a class of anionic clays that have attracted interest in many fields, specifically in environmental applications in recent years. LDH exhibits a sandwich-like structure, in which negative anions are cornered into positively charged metal layers in a repeating manner. The most important group of LDH may be represented by the formula [M<sub>1–x</sub><sup>2+</sup>M<sub>x</sub><sup>3+</sup>(OH)<sub>2</sub>]<sub>A<sub>x/n</sub></sub><sup>n–</sup>·mH<sub>2</sub>O, where M<sup>2+</sup> and M<sup>3+</sup>

<sup>a</sup>University of Coimbra, CERES, Department of Chemical Engineering, 3030-790 Coimbra, Portugal. E-mail: ines.borges@student.uc.pt; guida@eq.uc.pt

<sup>b</sup>Smallmatek – Small Materials and Technologies, Lda, 3810-075 Aveiro, Portugal

<sup>c</sup>CICECO-Aveiro Institute of Materials, Department of Chemistry, University of Aveiro, 3810-193 Aveiro, Portugal



are divalent and trivalent cations, respectively,  $x$  is equal to the ratio  $M^{3+}/(M^{2+} + M^{3+})$ , and  $A^{n-}$  is an anion of valence  $-n$ . Among many applications, the capture of P from liquid effluents has been considered in the literature.<sup>10–13</sup> For phosphorus recovery, LDH can be used directly or undergo a previous thermal treatment, such as calcination. During the heating process, there is a progressive loss of water, and the charge compensation anions present in the interlayer are removed, resulting in the collapse of the structure and formation of Layered Double Oxides (LDO) or mixed metal oxides.<sup>14</sup> According to previous studies, LDO can exhibit better performance as a sorbent material than LDH because, after calcination, there is a simultaneous increase in surface area and binding sites that promote anion intercalation.<sup>15</sup> When LDO is in contact with aqueous solutions, anions, and water molecules can be incorporated into the interlayer galleries, whereas water is sorbed to reconstruct the hydroxyl layers. This phenomenon, the conversion of LDO into LDH, has been reported as a “memory effect”.<sup>16–19</sup> Additionally, in this case, the release of anions into the aqueous medium is not observed.

Phosphorus removal from water matrices is currently a relevant research topic, and in the last few years, there has been a considerable number of published articles on this topic. Xueying Wang and co-workers used calcined Mg–Fe–La to remove phosphorus from real wastewater and achieved a decrease in phosphorus concentration from 3.6 to 0.12 mg L<sup>-1</sup>.<sup>20</sup> Ashekuzzaman and Jiang obtained 97–99% phosphate removal using a dose of 0.3 g L<sup>-1</sup> for the 10 mg L<sup>-1</sup> of P test solution by Ca-based LDH.<sup>21</sup> Kun Yang *et al.* achieved 97% phosphorus removal using ZnAlNO<sub>3</sub> by adding 0.04 g of LDH into 25 mL of 40 mg L<sup>-1</sup>.<sup>22</sup> Novillo and co-workers studied the removal capacity of MgAlNO<sub>3</sub> and concluded that at the optimum pH 3, the adsorption capacity was 71.2 mg L<sup>-1</sup>.<sup>23</sup> Zhou and co-authors reported that the sorption capacity of ZnAl-LDH tripled when the material was calcined because of the release of carbonate ions from the interlayer space, producing more active sites for phosphorus capture during the rehydration process.<sup>24</sup> The use of these materials for P removal has yielded encouraging outcomes, and various chemical compositions have been tested. In most cases, the materials employed were synthesized on a laboratory scale. Scaling up would be significantly more straightforward if the materials had an established production process and a market price that was competitive with other products on the market. An innovative contribution of the present study is the evaluation of the performance of selected commercial materials. In addition, it is worth highlighting that several studies have indicated calcination to be an effective method for enhancing the sorption capacities of LDH. However, it is imperative to undertake a meticulous analysis of the application of this process, given the substantial financial implications involved.

This work aims to evaluate LDH (ZnAlNO<sub>3</sub>) and LDO (ZnAl-LDO and MgAl-LDO) as sorbent materials for phosphorus recovery from aqueous synthetic matrices, with the goal of selecting the most effective material for further testing in a pilot-scale process. The key contribution of this study is to demonstrate the potential of industrial-scale materials for

phosphorus removal, supporting the feasibility of large-scale applications. Furthermore, both ZnAlNO<sub>3</sub> and its calcined form, ZnAl-LDO, were tested to investigate whether calcination increases the sorption capacity. MgAlCO<sub>3</sub>, a commercial material, was also calcined into its MgAl-LDO form for comparison.

## 2. Materials and methods

### 2.1. Materials and characterization

In this study, three materials were selected for testing and comparing their phosphorous-removing capacity from aqueous matrices. The selected materials are hydrotalcite (MgAlCO<sub>3</sub>) in its calcined form (*i.e.*, MgAl-LDO), ZnAlNO<sub>3</sub>, and its calcined form ZnAl-LDO. The MgAlCO<sub>3</sub> was purchased from KISUMA Chemicals (The Netherlands) whereas commercial ZnAlNO<sub>3</sub> LDH was produced by Smallmatek, Lda, through the coprecipitation method. The synthesis was performed by gradually adding 0.5 M Zn(NO<sub>3</sub>)<sub>2</sub> · 6H<sub>2</sub>O and 0.25 M Al(NO<sub>3</sub>)<sub>3</sub> · 9H<sub>2</sub>O solutions to a 1.5 M NaNO<sub>3</sub> under continuous stirring at room temperature. Throughout the reaction, the pH was maintained 9.5 ± 0.5 by the controlled addition of a 2 M NaOH solution. The production process was carried out in a custom-made stainless-steel reactor (BTL-Indústrias Metalúrgicas, S.A., Oliveira de Azeméis, Portugal) equipped with an automatic pH control system using a PDA controller. After reaction, a hydrothermal treatment was performed in the reactor at 100 °C. Both materials were calcined at 650 °C for 4 hours and milled to obtain a fine powder ( $d_{90} < 25 \mu\text{m}$ ).<sup>25–27</sup> It must be mentioned that Mg-based LDH was tested only in its calcined form mainly due to two reasons: the stability of CO<sub>3</sub><sup>2-</sup> in the LDH interlayer region penalizes the anionic exchange capacity of MgAlCO<sub>3</sub>,<sup>28</sup> and the presence of fatty acids on the surface (of this commercial material) increases the hydrophobicity, which limits its application in aqueous matrices. KH<sub>2</sub>PO<sub>4</sub>, supplied by Panreac (≥99%), was used as the phosphorus source in all sorption experiments.

The starting materials (LDH and LDO) were characterized in terms of specific surface area and particle size distribution. Nitrogen adsorption-desorption isotherms were used to measure the specific surface area ( $A_{\text{BET}}$ ) after the sample had been degassed overnight under vacuum and was obtained using a Micromeritics Gemini V-2380.<sup>29</sup> Particle size distribution was determined using a Mastersizer 2000. The samples were dispersed in Tween 80 and then exposed to ultrasounds for 1–3 minutes to ensure particle disaggregation. The mineral phase content and crystal structure of the samples were characterized by X-ray diffraction (XDR) using a MiniFlex 600 benchtop X-ray diffractometer and filtered CuK $\alpha$  radiation. The measurements were performed in the 2 $\theta$  mode, using a bracket sample holder with a scanning speed of 10° min<sup>-1</sup> in continuous mode over the range from 3° to 65°. Fourier transform infrared spectroscopy (FTIR) with ATR unit (diamond crystal) was used to analyze the functional groups at 8 cm<sup>-1</sup> of the resolution, from 4000 to 400 cm<sup>-1</sup>, with 64 scans, on a PerkinElmer FTIR Spectrometer, Spectrum Two. The pH of suspensions was measured using a HI 2550 multiparameter from HANNA Instruments.



## 2.2. Batch equilibrium and kinetic tests

The P removal capacity (RE) of MgAl-LDO, ZnAl-LDO, and ZnAlNO<sub>3</sub> was determined by adding 1 g of sorbent to 100 mL of a synthetic solution containing 100 mg L<sup>-1</sup>, under mechanical agitation at *T* = 25 °C for 24 hours. It is then calculated by:

$$RE = 100 \frac{C_i - C_f}{C_f} \quad (1)$$

where *C<sub>i</sub>* and *C<sub>f</sub>* are the initial and final P concentrations (mg L<sup>-1</sup>), respectively.

The sorption kinetic tests of phosphate on ZnAlNO<sub>3</sub> were performed in batch conditions for an initial phosphorus concentration of 100 mg L<sup>-1</sup> using dosages ranging from 0.25 to 2 g L<sup>-1</sup>. At appropriate time intervals, aliquots were withdrawn using a plastic syringe, and the samples were immediately filtered through a 0.22 μm pore-size cellulose nitrate filter. The adsorption isotherms were obtained using a method similar to that described for the kinetic studies and lasted 24 hours.

To determine the mechanisms involved in the sorption of phosphorus, four mathematical models were tested to fit the experimental data: pseudo-first-order, pseudo-second-order, Elovich, and intra-particle diffusion models. To perform the linear fitting of these models, they should be, respectively, expressed by:

$$\ln(q_e - q_t) = \ln q_e - k_1 t \quad (2)$$

$$\frac{t}{q} = \frac{1}{k_2 q_e^2} + \frac{1}{q_e} t \quad (3)$$

$$q_t = \frac{1}{\beta} \ln(\alpha\beta) + \frac{1}{\beta} \ln(t) \quad (4)$$

$$q_t = k_i \times t^{0.5} + C \quad (5)$$

where *q<sub>e</sub>* and *q<sub>t</sub>* (mg g<sup>-1</sup>) are the concentrations of phosphorus sorbed on the materials at equilibrium and at time *t* (min), respectively; the rate constants of pseudo-first and pseudo-second-order are *k<sub>1</sub>* (min<sup>-1</sup>) and *k<sub>2</sub>* (g mg min<sup>-1</sup>), respectively, *α* is the initial adsorption rate (mg g<sup>-1</sup>), *β* is the desorption constant (g mg<sup>-1</sup>), *k<sub>i</sub>* is the intra-particle diffusion rate constant (mg g<sup>-1</sup> h<sup>-0.5</sup>), and *C* is a constant (mg g<sup>-1</sup>).<sup>22,30,31</sup>

The experimental equilibrium data were fitted by the Langmuir and Freundlich isotherms, whose linearized forms are given by, respectively:

$$\frac{C_e}{q_e} = \frac{1}{q_m K_L} + \frac{C_e}{q_m} \quad (6)$$

$$\ln q_e = \ln k_F + \frac{1}{n} \ln C_e \quad (7)$$

where *q<sub>e</sub>* (mg g<sup>-1</sup>) and *C<sub>e</sub>* (mg L<sup>-1</sup>) are the equilibrium concentrations of P in the solid material and solution, respectively, *q<sub>e</sub>* and *K<sub>L</sub>* are the Langmuir parameters, and *k<sub>F</sub>* is the Freundlich constant.

The equilibrium concentration in the solid is calculated by:

$$q_e = \frac{(C_i - C_e)}{D} \quad (8)$$

where *C<sub>i</sub>* and *C<sub>e</sub>* are the initial and equilibrium concentrations, respectively, and *D* is the dosage (g L<sup>-1</sup>) of sorbent used in the batch tests. The phosphate concentration in the solution was determined at a wavelength of 650 nm using the 365.3 EPA method.<sup>32</sup> A VWR UV-1600PC Spectrophotometer was employed. Three replicates were performed for each sample, and the standard deviation of errors was calculated and reported in each case.

To evaluate the material integrity, samples were immersed in a 100 mg L<sup>-1</sup> of phosphorus solution and stirred continuously for 5 days at 400 rpm. After this period, an external laboratory analyzed the concentrations of Zn, Al, and Mg using inductively coupled plasma mass spectrometry (ICP-MS), and the results were expressed per gram of LDH. The measured Zn leaching was 164 mg g<sup>-1</sup> for ZnAl-LDO and 9.90 mg g<sup>-1</sup> for ZnAl-NO<sub>3</sub>. The detected concentrations of Al were 0.164 mg g<sup>-1</sup> for ZnAl-LDO, 3.53 mg g<sup>-1</sup> for ZnAl-NO<sub>3</sub>, and 167 mg g<sup>-1</sup> for MgAl-LDO. In the case of MgAl-LDO, the Mg release was 6.30 × 10<sup>-4</sup> mg g<sup>-1</sup>.

## 3. Results and discussion

### 3.1. Structural and morphological characterization of LDH and LDO materials

The specific surface areas and particle size distributions of the materials were determined, and the results are summarized in Table 1.

The particle size distribution of ZnAlNO<sub>3</sub> and ZnAl-LDO in terms of *d*<sub>10</sub>, *d*<sub>50</sub>, *d*<sub>90</sub> ranges from 1.852–18.94 and 0.7760–24.14 μm, respectively, illustrating some heterogeneity in the materials. The particle size and its distribution might affect the sorption performance of the materials, as well as the reproducibility of the tests. Calcination is a common post-synthesis treatment used with LDH, often presented in the literature as a method for increasing the specific surface area of the material, potentially resulting in a higher sorption capacity.<sup>7,18</sup> As mentioned previously, MgAlCO<sub>3</sub> hydrotalcite is a commercially available product, and according to the information provided by the supplier its surface area is 8 m<sup>2</sup> g<sup>-1</sup>. Thus, in this case, calcination results in a material with a higher surface area (*i.e.*, 18.52 m<sup>2</sup> g<sup>-1</sup>). However, based on the results presented in Table 1, the ZnAl-LDO did not exhibit any improvement in the specific surface area when compared to ZnAlNO<sub>3</sub>. The specific surface area of the material after calcination depends on several parameters, including calcination temperature, metal ratio, and intercalated anions in the initial LDH structure. MgAl-LDO has

**Table 1** Specific surface area and particle size distribution (in terms of *d*<sub>10</sub>, *d*<sub>50</sub>, *d*<sub>90</sub>) of MgAlCO<sub>3</sub>, MgAl-LDO, ZnAlNO<sub>3</sub>, and ZnAl-LDO

Sample	<i>A</i> <sub>BET</sub> (m <sup>2</sup> g <sup>-1</sup> )	<i>d</i> <sub>10</sub> (μm)	<i>d</i> <sub>50</sub> (μm)	<i>d</i> <sub>90</sub> (μm)
MgAlCO <sub>3</sub>	8.0 <sup>a</sup>	0.5 <sup>a</sup>	0.7 <sup>a</sup>	0.8 <sup>a</sup>
MgAl-LDO	18.52	0.4040	1.313	3.704
ZnAlNO <sub>3</sub>	17.32	1.852	6.277	18.94
ZnAl-LDO	14.74	0.7760	4.119	24.14

<sup>a</sup> Provided by the supplier of the material.



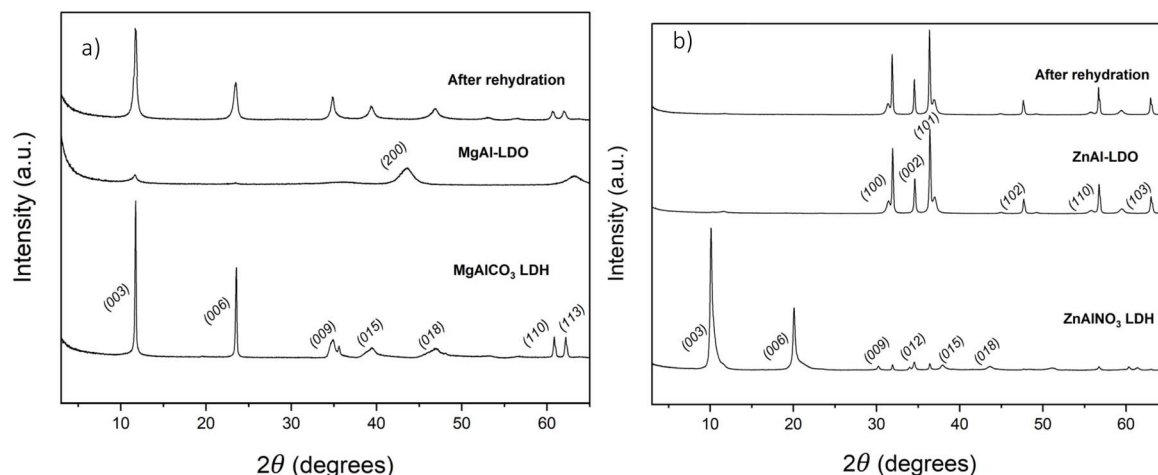


Fig. 1 XRD of (a)  $\text{MgAlCO}_3$  and (b)  $\text{ZnAlNO}_3$  before and after calcination, and after the rehydration process.

a slightly higher surface area than  $\text{ZnAl-LDO}$ , which could be related to the surface energy of the divalent metal oxides ( $\text{MgO}$  or  $\text{ZnO}$ ).<sup>34</sup> Preliminary studies confirmed that the calcination temperature should be *ca.* 650 °C. However, some authors have suggested that calcination above 600 °C does not result in a higher surface area and sometimes leads to the formation of spinels, which directly affects the reconstruction process of LDH. The temperature required for spinel phase formation varies in the literature.<sup>14,20,34,35</sup> One of the advantages of using calcined materials is that their structure collapses, and thus, when used as a sorbent material, there is no release of anions into the liquid medium. Additionally, some studies have reported an increase in specific surface area (and porosity), which may improve the sorption capacity. To determine whether the materials could reacquire their initial structures, 50 mg of the calcined material was placed in contact with 100 mL of distilled water for 24 hours, under stirring. After this period, the solution was filtered, and the materials were dried and analyzed by XRD (Fig. 1).

Fig. 1a shows that calcination destroyed the  $\text{MgAlCO}_3$  LDH structure, while (200) reflections typical of oxide metals are present in  $\text{MgAl-LDO}$ . After 24 hours of contact with distilled water,  $\text{MgAl-LDO}$  reacquired its initial structure, indicating that if its use is considered for continuous applications, the material will attain the LDH structure within a short time. The XRD pattern in Fig. 1b shows that, after calcination,  $\text{ZnAlNO}_3$  lost the initial structure of the LDH, and the typical peaks of metal-mixed oxides appeared at (100), (002), (101), (102), (110), and (103). However, in this case, after 24 hours in aqueous solution, the  $\text{ZnAl-LDO}$  was not able to reacquire the LDH structure. Thus, for  $\text{ZnAlNO}_3$ , the oxide structure was preserved. Although it did not exhibit an increased surface area after calcination, the sorption capacities of both calcined and non-calcined materials were further evaluated.

### 3.2. Screening of materials

After evaluating the “memory effect”, the three materials under study ( $\text{MgAl-LDO}$ ,  $\text{ZnAlNO}_3$ , and  $\text{ZnAl-LDO}$ ) were assessed for

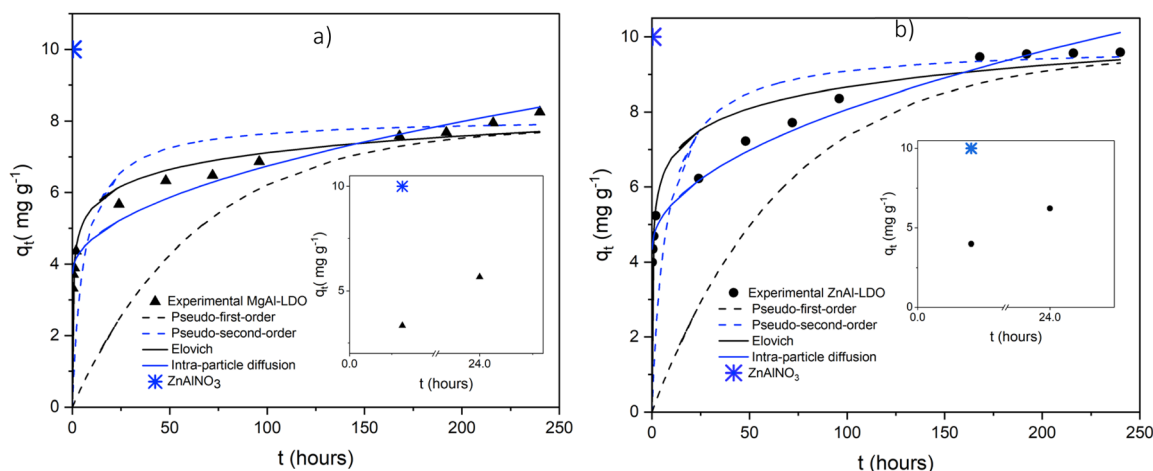


Fig. 2 Effect of contact time on the phosphorus sorption by (a)  $\text{MgAl-LDO}$  and (b)  $\text{ZnAl-LDO}$ . Symbols represent experimental data ( $D = 10 \text{ g L}^{-1}$ ,  $C_i = 100 \text{ mg L}^{-1}$ ) while the curves correspond to the predictions through pseudo-first-order, pseudo-second-order, Elovich, and intra-particle diffusion models. The insets in each figure provide an enlarged view, highlighting the experimental point for  $\text{ZnAlNO}_3$  measured at  $t = 0.2 \text{ h}$ .





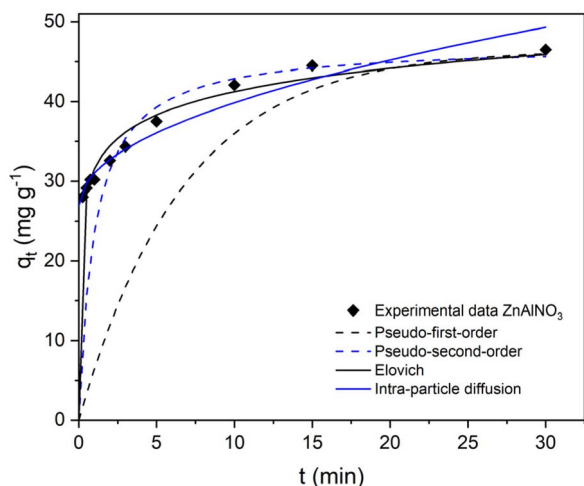


Fig. 3 Kinetic study of P removal using  $\text{ZnAlNO}_3$ . Symbols are experimental data ( $D = 10 \text{ g L}^{-1}$ ,  $C_i = 500 \text{ mg L}^{-1}$ ), and the curves correspond to the pseudo-first, pseudo-second, Elovich, and intra-particle diffusion models.

their adsorption properties. Thus, to select the material with the greatest potential, the removal capacity was measured as a function of time at a dose of  $10 \text{ g L}^{-1}$  and a constant initial P concentration of  $100 \text{ mg L}^{-1}$ . Fig. 2a and b depict the P removal kinetics of MgAl-LDO and ZnAl-LDO, respectively. The  $\text{ZnAlNO}_3$  sorption capacity was also evaluated and is presented in the two insets in Fig. 2 to compare the performance of non-calcined and calcined forms.

The performance of  $\text{ZnAlNO}_3$  LDH stands out when compared with the calcined LDO because it was able to remove 100% of the phosphorus present in the solution after the first 15 minutes, which means that the kinetics is much faster than in the calcined forms. Focusing on calcined materials, the profiles observed show that the uptake of P is relatively fast in the first hours (reaching  $\sim 50\%$  of removal) but continues to increase slowly over 10 days (240 hours). These results indicate that phosphorus sorption onto LDO may involve different mechanisms compared to LDH. In this regard, it is important to note that most studies have assumed that equilibrium is reached

within the first 24 hours.<sup>7,33,36</sup> However, Chitrakar *et al.* also reported slow kinetics for the calcined product of  $\text{MgMnCO}_3$  in the seawater system. In this case, the equilibrium concerning phosphorus concentration was reached after three days, despite 70% of P being removed in the first 24 hours.<sup>37</sup> Indeed, the removal was faster in the first three days, but a decline in the sorption rate was then observed due to a decrease in the concentration driving force for adsorption.

The study carried out with  $\text{ZnAlNO}_3$  revealed that it could remove approximately  $100 \text{ mg L}^{-1}$  within 15 minutes. Therefore, to evaluate the uptake kinetics for this material, another experiment was performed with a dose of  $10 \text{ g L}^{-1}$ , but with an initial concentration of  $500 \text{ mg L}^{-1}$ . Fig. 3 displays the kinetic profile obtained with  $\text{ZnAlNO}_3$  and the fittings of the four kinetic models. In this case, the capacity of the LDH as time approaches 30 min was  $46.5 \text{ mg g}^{-1}$ , corresponding to a removal efficiency of 93%. The maximum sorption capacity experimentally obtained for MgAl-LDO, ZnAl-LDO, and  $\text{ZnAlNO}_3$  was 8.26, 9.59, and  $46.5 \text{ mg g}^{-1}$ , respectively, which means that the sorption capacity of  $\text{ZnAlNO}_3$  is approximately five times higher than that of the calcined form and approximately six times higher than that of MgAl-LDO. The kinetic parameters of the applied models (eqn (2)–(5)) for MgAl-LDO, ZnAl-LDO, and  $\text{ZnAlNO}_3$  are listed in Table 2.

A comparison of the kinetic models, in terms of the coefficient of determination ( $R^2$ ), revealed that the pseudo-second-order model was the most suitable for describing the sorption kinetics of phosphate on these materials, which follows previous literature.<sup>33,38</sup> According to the assumptions underlying the model, the phosphate adsorption process is governed by chemisorption, *i.e.* chemical bonding between the sorbent active sites and phosphate.<sup>36,39</sup> The  $k_2$  rate constants of the calcined and non-calcined materials differ by three orders of magnitude, revealing that the  $\text{ZnAlNO}_3$  is characterized by significantly faster kinetics, clarifying why it was not possible to conduct a proper kinetic study using  $10 \text{ g L}^{-1}$  and  $100 \text{ mg L}^{-1}$ . The intra-particle diffusion constant,  $C$ , is nonzero for any of the tested materials, which leads to the conclusion that the diffusion is not the only rate-controlling step.<sup>33,40,41</sup> The Elovich model also provides a reasonable fit for kinetic data and is likely

Table 2 Kinetic parameters of the tested models to describe phosphorus sorption on MgAl-LDO, ZnAl-LDO, and  $\text{ZnAlNO}_3$

Kinetic model		MgAl-LDO <sup>a</sup>	ZnAl-LDO <sup>a</sup>	$\text{ZnAlNO}_3$ <sup>b</sup>
Pseudo-first-order	$q_e (\text{mg g}^{-1})$	7.87	9.59	46.5
	$k_1 (\text{min}^{-1})$	$2.60 \times 10^{-4}$	$2.43 \times 10^{-4}$	0.371
	$R^2$	0.988	0.982	0.889
Pseudo-second-order	$q_e (\text{mg g}^{-1})$	8.09	9.76	47.2
	$k_2 (\text{g (mg min)}^{-1})$	$3.54 \times 10^{-4}$	$2.34 \times 10^{-4}$	0.0212
	$R^2$	0.995	0.994	0.998
Elovich	$\alpha (\text{mg (g min)}^{-1})$	4.07	4.12	7309
	$\frac{1}{\beta} (\text{mg g}^{-1})$	0.678	0.825	4.23
	$R^2$	0.969	0.943	0.955
Intra-particle diffusion model	$k_i$	0.0388	0.0481	4.08
	$C$	3.74	4.34	26.9
	$R^2$	0.969	0.980	0.951

<sup>a</sup> Experiments with  $C_i = 100 \text{ mg L}^{-1}$  and  $D = 10 \text{ g L}^{-1}$ . <sup>b</sup> Experiments with  $C_i = 500 \text{ mg L}^{-1}$  and  $D = 10 \text{ g L}^{-1}$ .

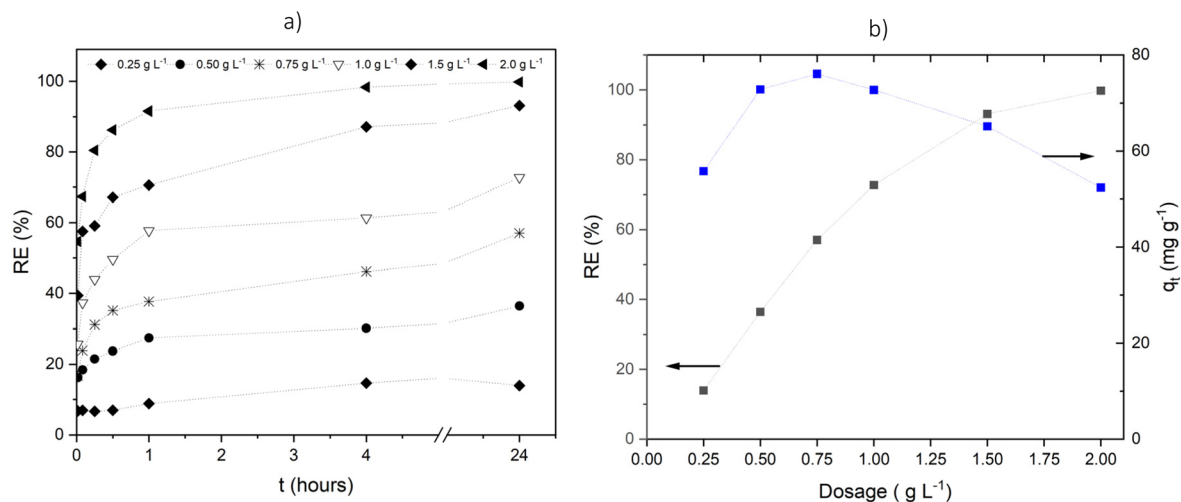


Fig. 4 Phosphorus removal using  $\text{ZnAlNO}_3$  and initial solution concentration  $C_i = 100 \text{ mg L}^{-1}$ : (a) Removal efficiency over time for different sorbent dosages. (b) Removal efficiency (left axis) and solid concentration (right axis) as a function of sorbent dosages at  $t = 24$  hours.

to involve chemisorption.<sup>42,43</sup> Based on the Elovich model constants, it can be concluded that the sorption process was very fast for  $\text{ZnAlNO}_3$  with a value of  $\alpha = 7309 \text{ mg g}^{-1} \text{ min}^{-1}$ .

The intercept term  $\frac{1}{\beta} \ln(\alpha\beta)$  provides the total amount sorbed after 1 minute. In this case, intercept value is 31.52, which corresponds to 68% of the total phosphorus removed in 1 minute and highlights the high velocity of the process.<sup>40</sup> For  $\text{MgAl-LDO}$  and  $\text{ZnAl-LDO}$ , the intercept values are 1.21 and 1.40, which corresponds to approximately 15% of the total phosphorus captured by both.

Based on the results obtained in this screening step,  $\text{ZnAlNO}_3$  is the material with the best performance for removing phosphorus from aqueous matrices, and thus a more detailed study was conducted in the following sections.

### 3.3. Effect of the sorbent dosage on the performance of $\text{ZnAlNO}_3$

The effect of dosage on phosphorus removal was investigated using  $\text{ZnAlNO}_3$ , the most effective sorbent, over the range of

0.25 to  $2 \text{ g L}^{-1}$ , while maintaining the initial P concentration at  $100 \text{ mg L}^{-1}$ . Fig. 4a shows the removal efficiency as a function of LDH dosage for 24 hours, while Fig. 4b depicts the removal efficiency (RE) after 24 hours of experiment and the respective solid concentration,  $q_t$  ( $\text{mg g}^{-1}$ ), as a function of LDH dosage.

As expected, the removal efficiency of the material increased as the dosage increased, reaching >99% at a dosage of  $2 \text{ g L}^{-1}$ . The amount of phosphorus that was uptaken in the first hour is higher for higher dosages, which is related to the higher amount of available sorption sites. At a low fraction of sorbent, all types of sites are fully exposed to the interactions, leading to rapid surface saturation.<sup>23,44</sup> As illustrated in Fig. 4b, after 24 hours, the amount of sorbed P increases with the increasing amount of sorbent from  $0.25$  to  $2 \text{ g L}^{-1}$ , but the loading capacity increases for dosages until  $0.75 \text{ g L}^{-1}$ , then decreases. Based on the kinetic study, using  $0.75 \text{ g L}^{-1}$  of  $\text{ZnAlNO}_3$ , the loading capacity was  $76 \text{ mg g}^{-1}$ . This analysis emphasizes how crucial dosage selection is, as it must take into account effective removal without diminishing material loading. For example,

Table 3 Parameters of a kinetic model to describe phosphorus sorption on  $\text{ZnAlNO}_3$  using different dosages

Kinetic model							
Dosage	$\text{g L}^{-1}$	0.25	0.5	0.75	1.0	1.5	2
Pseudo-first-order	$q_e$ ( $\text{mg g}^{-1}$ )	41.9	31.3	39.4	30.5	26.0	13.5
	$k_1$ ( $\text{min}^{-1}$ ) $\times 10^{-3}$	8.10	3.50	3.70	3.70	6.30	1.12
	$R^2$	0.983	0.856	0.884	0.753	0.933	0.948
Pseudo-second-order	$q_e$ ( $\text{mg g}^{-1}$ )	56.5	73.0	76.3	73.0	65.4	52.4
	$k_2$ ( $\text{g (mg min)}^{-1}$ ) $\times 10^{-3}$	2.29	0.639	0.502	0.710	1.32	5.55
	$R^2$	0.999	0.998	0.998	0.998	0.999	0.999
Elovich	$\alpha$ ( $\text{mg (g min)}^{-1}$ )	134	980	129	448	$1.21 \times 10^3$	$2.89 \times 10^4$
	$\frac{1}{\beta}$ ( $\text{mg g}^{-1}$ )	5.80	5.73	7.41	6.39	5.32	3.47
	$R^2$	0.723	0.981	0.997	0.984	0.972	0.920
Intra-particle diffusion model	$k_i$	1.04	1.02	1.29	1.06	0.878	0.505
	$C$	28.2	39.5	34.4	39.2	39.0	38.6
	$R^2$	0.627	0.836	0.813	0.726	0.712	0.526

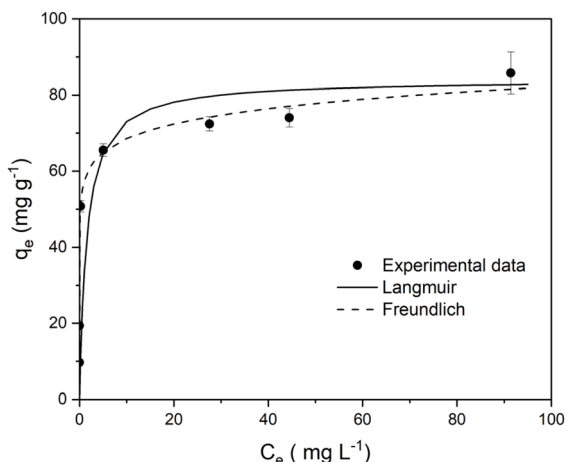


Fig. 5 Sorption isotherm of phosphorus by  $\text{ZnAlNO}_3$  ( $C_i = 100 \text{ mg L}^{-1}$ ,  $T = 25^\circ\text{C}$ ,  $\text{pH}_i = 5.25$ ,  $D = 0.10, 0.75, 1.0, 1.5, 2.0, 5.0, 10 \text{ g L}^{-1}$ ).

using a dosage of  $1 \text{ g L}^{-1}$  instead of  $0.75 \text{ g L}^{-1}$  will improve the removal efficiency from 57% to 73%.

The parameters obtained by fitting the pseudo-first-order, pseudo-second-order, Elovich, and intra-particle diffusion models to the experimental data are listed in Table 3.

As previously mentioned, the pseudo-second-order model is the one that better describes phosphorus capture on  $\text{ZnAlNO}_3$  and also the one where the coefficient of determination is closer to 1 in all dosages studied. The  $R^2$  values obtained by fitting the intra-particle model were quite low for almost all dosages owing to the multilinearity of the plot, suggesting that there is more than one mechanism involved in phosphorus removal, which is in accordance with other published works.<sup>23,24,33</sup>

Table 4 Sorption isotherm parameters of  $\text{ZnAlNO}_3$

Model	Parameters	
Langmuir $\frac{C_e}{q_e} = \frac{1}{q_m K_L} + \frac{C_e}{q_m}$	$q_m \text{ (mg g}^{-1}\text{)}$	84.0
	$K_L \text{ (L mg}^{-1}\text{)}$	0.665
	$R^2$	0.993
Freundlich $\ln q_e = \ln K_F + \frac{1}{n} \ln C_e$	$K_F \text{ (mg g}^{-1} \text{ (L mg}^{-1}\text{)}^{-1/n}\text{)}$	57.3
	$n$	12.8
	$R^2$	0.968

Table 5 Comparison of literature and present study on phosphorus uptake from aqueous solutions

Sorbent	Dosage ( $\text{g L}^{-1}$ )	Initial P concentration ( $\text{mg L}^{-1}$ )	Maximum sorption capacity ( $\text{mg g}^{-1}$ )	Reference
$\text{ZnAlNO}_3$ (3 : 1)	3.0	33.3	34.2	11
$\text{ZnAlNO}_3$ (1.25 : 1)	1.0	100	90.1	33
$\text{ZnAlNO}_3$	0.40	3.30–97.8	24.8	24
ZnAl-LDO	0.40	3.30–97.8	75.6	24
MgAl-LDO	1.0	16.7	14.7	44
MgAl-LDO	5.0	33.0–65.0	29.1	46
$\text{ZnAlNO}_3$ (2 : 1)	10	500	47.2	This study
$\text{ZnAlNO}_3$ (2 : 1)	0.10	100	84.0	This study
ZnAl-LDO	10	100	9.76	This study
MgAl-LDO	10	100	8.09	This study

### 3.4. Equilibrium studies on $\text{ZnAlNO}_3$

The most commonly used adsorption equilibrium models are the Langmuir and Freundlich equations. In contrast to the Freundlich model (initially established as an empirical equation and then derived for material with heterogeneous surfaces or either ion exchange applications) which is frequently used to describe chemisorption on heterogeneous surfaces, the Langmuir model assumes monolayer adsorption on a homogeneous surface with no interactions between the sorbed molecules.<sup>23</sup> The adsorption isotherm of  $\text{ZnAlNO}_3$  is shown in Fig. 5, where loading capacity,  $q_e \text{ (mg g}^{-1}\text{)}$ , is plotted as a function of equilibrium concentration,  $C_e \text{ (mg L}^{-1}\text{)}$ , reached after 24 hours of exposure. The equilibrium parameters obtained by fitting the Langmuir and Freundlich models are listed in Table 4.

Based on the coefficient of determination,  $R^2$ , the Langmuir model best described the phosphate sorption data. The maximum loading capacity of  $\text{ZnAlNO}_3$ , as determined by the Langmuir model, was  $84 \text{ mg g}^{-1}$ . According to this isotherm, adsorption occurs in a monolayer on specific active sites, with uniform adsorption energy and no interaction between adsorbed solutes. When the Langmuir model is valid, the dimensionless equilibrium parameter  $R_L$ , also known as the separation factor, can be calculated to predict the favorability of the sorption process,<sup>31,33,45</sup>

$$R_L = \frac{1}{1 + K_L C_i} \quad (9)$$

where  $C_i \text{ (mg L}^{-1}\text{)}$  is the initial concentration and  $K_L \text{ (L mg}^{-1}\text{)}$  is the Langmuir constant. In general, if  $R_L = 0$ , the adsorption is considered irreversible; for  $0 < R_L < 1$  adsorption is favorable and reversible; if  $R_L = 1$ , the behavior is linear; and unfavorable for  $R_L > 1$ . In the present study,  $R_L = 0.0148$ , which means that the adsorption process is favorable. Table 5 presents a comparison of literature and present study results on phosphorus uptake from aqueous solutions. Considering these results, it can be concluded that the capacity of the calcined materials in this study is lower to that previously documented in the literature. Thus, the calcination process did not yield the expected improvements. However,  $\text{ZnAlNO}_3$ , despite exhibiting metal ratios that differ from those reported in the literature, demonstrated performance consistent with the scope of the studied presented in Table 5.



### 3.5. Influence of dosage on phosphorus capture and its impact on LDH structure

During the equilibrium and kinetic experiments, a standard protocol was implemented wherein post-exposure LDH samples were systematically characterized by XRD. This analysis aimed to verify the intercalation of phosphate ions and to evaluate the resulting structural modifications in the LDH. The findings indicated that the final LDH structure was influenced by the dosage levels applied during the tests. Fig. 6 summarizes the XRD pattern of LDH before and after the sorption tests using different dosages, while in Fig. 7 three possible scenarios for phosphate capture by  $\text{ZnAlNO}_3$  are proposed.

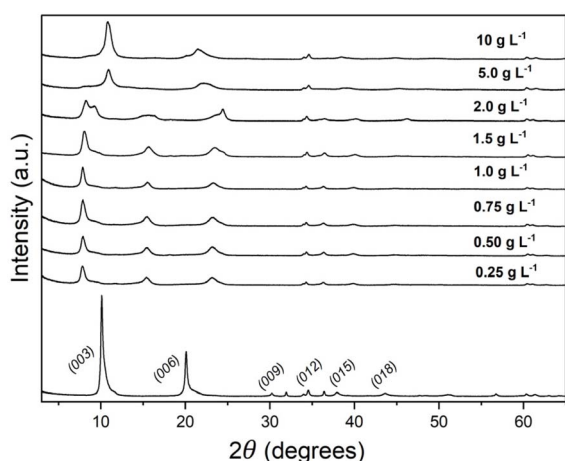


Fig. 6 XRD analysis of  $\text{ZnAlNO}_3$  before and after the sorption batch test at dosages of 0.25, 0.5, 0.75, 1.0, 1.5, 2.0, 5.0, and  $10 \text{ g L}^{-1}$ .

All tests were conducted at a pH of approximately 5 (the pH of the  $\text{KH}_2\text{PO}_4$  solution used in assays with  $[\text{P}] = 100 \text{ mg L}^{-1}$ ), where phosphorus predominantly occurs as  $\text{H}_2\text{PO}_4^-$ , which is likely the species preferentially intercalated into the LDH gallery.

In the case of high LDH dosages ( $5$  and  $10 \text{ g L}^{-1}$ ), as discussed above, there was a total removal of phosphorus present in the solution, and it can be concluded that the dosages were overestimated, which means that the material was not used to its full potential. Since the ratio of material/solution is high, the amount of  $\text{H}_2\text{PO}_4^-$  into the LDH galleries is much lower when compared to the amount of  $\text{NO}_3^-$ , a small readjustment of LDH structure occurred leading to a small shift of (003) reflection to higher 2 theta angles, as observed in Fig. 6 and proposed in Fig. 7 (Scenario 1). This readjustment can occur up to the point where the occupied volume by phosphates is closer to the nitrates volume in the gallery (*i.e.* the concentration difference between phosphates and nitrates is smaller). In the case of low LDH dosages, there is a clear shift of the (003) reflection to lower 2 theta angles (Fig. 6), which indicates that basal space increased due to the high presence of phosphates, confirming a successful intercalation, *i.e.* most nitrate anions were replaced by phosphorous species as proposed on Fig. 7 (Scenario 2). For intermediate dosages, between  $0.75$ – $2 \text{ g L}^{-1}$ , the (003) reflection also shifts to lower 2 theta angles, as can be seen in Fig. 6, showing that when the amount of phosphates and nitrates are closer, the prevailing volume is from phosphates.

To the best of our knowledge, this is the first time that the impact of dosage on LDH structure after sorption tests has been reported. Although the main objective of this work is the

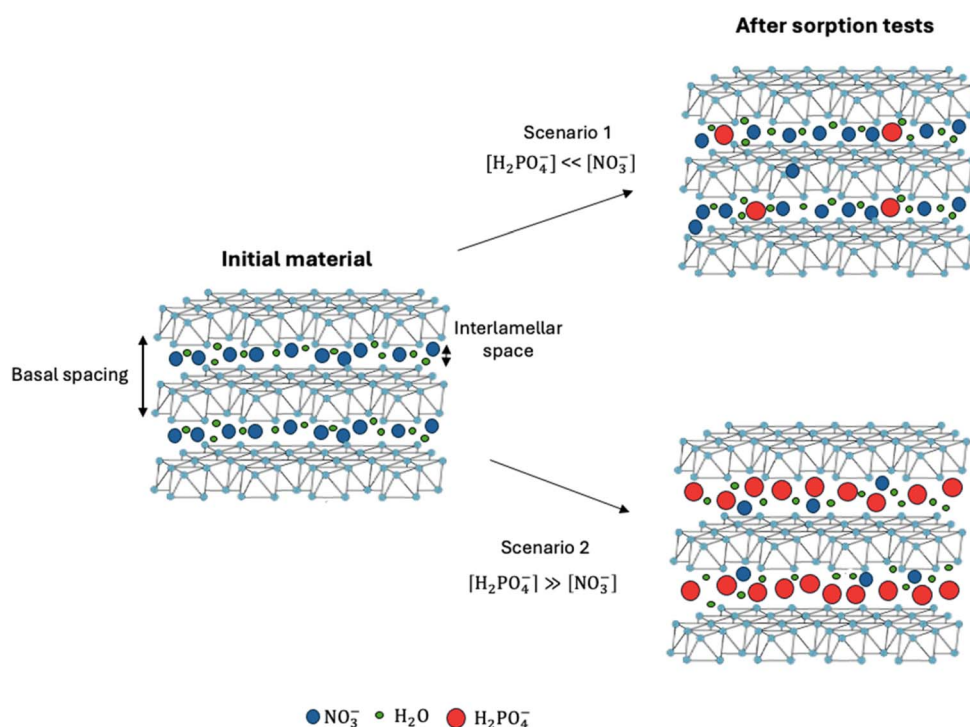


Fig. 7 Changes occurring in the structure of  $\text{ZnAlNO}_3$  in three different scenarios for phosphate capture.





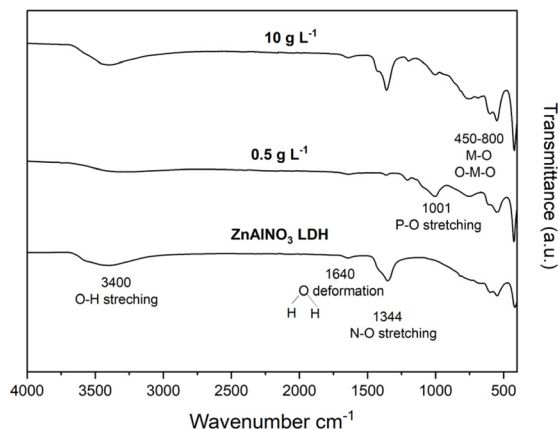


Fig. 8 FTIR analysis of  $\text{ZnAlNO}_3$  powder before and after sorption of phosphorus at two different dosages ( $0.5$  and  $10 \text{ g L}^{-1}$ ).

capture of phosphate using LDH, it is also very important to understand the way how phosphates are removed from the solution. In the future, more thorough research on this topic should be conducted.

The phosphorus sorption process was confirmed through FTIR spectroscopy, as shown in Fig. 8, supporting the XRD data.

Some of the characteristic bands of LDH are present in the starting material, namely a wide band around  $3400 \text{ cm}^{-1}$  could be attributed to O–H stretching vibration due to the presence of hydroxyl groups in the LDH structure or even due to some water molecules on the surface or present in the interlayer. A band near  $1640 \text{ cm}^{-1}$  featured the deformation vibration mode of OH bonds in water molecules. The most outstanding band is attributed to the stretching vibration of N–O at  $1344 \text{ cm}^{-1}$  since nitrate is the anion species intercalated in these LDH. Other bands that usually appear in low wave numbers ( $450\text{--}800 \text{ cm}^{-1}$ ) can be assigned to the lattice vibration modes of metal–oxide connections (O–M–O and M–O). In both cases, after sorption, bands corresponding to the P–O stretching vibration at  $1001 \text{ cm}^{-1}$  appeared, confirming the presence of phosphorus in the material. Although it was possible to remove all phosphorus present in the solution when using a dosage of  $10 \text{ g L}^{-1}$ , the band corresponding to nitrate was still very evident.<sup>23,36,47–49</sup>

## 4. Conclusions

This study aimed to evaluate the phosphorus recovery from aqueous matrices using LDH,  $\text{ZnAlNO}_3$ , and two calcined materials,  $\text{ZnAl-LDO}$  and  $\text{MgAl-LDO}$ . One of the advantages of submitting LDH to calcination is the collapsing of the lamellar structure. Thus, the release of the interlayer anion to the liquid during sorption is avoided and the anion of interest (phosphate) is captured. The results showed that, in contrast to  $\text{ZnAl-LDO}$ , the  $\text{MgAl-LDO}$  recovered its initial structure upon contact with water. However, both calcined forms revealed a lower capacity for recovering phosphate from the solution, when compared to the original LDH. Besides the lower sorption capacity of calcined materials, they exhibited very slow kinetics. On the other side,  $\text{ZnAlNO}_3$  shows faster kinetic and higher

performance when compared to the calcined forms. A deeper study was performed for  $\text{ZnAlNO}_3$ , where the sorption isotherm and kinetic data were best fitted by the Langmuir and pseudo-second-order models, respectively. The estimated maximum P-sorption capacity was  $84 \text{ mg g}^{-1}$ . Thus,  $\text{ZnAlNO}_3$  seems to be a promising sorbent for the safe and cost-effective removal of phosphate ions. It was also demonstrated for the first time that the LDH dosage used for P capture affects the final LDH structure, with two scenarios proposed based on the amounts of phosphates and nitrates present in the LDH interlamellar space. The regeneration tests coupled with these materials show good results. However, since the goal is to use the materials in a fertilizer solution, the sorption–desorption cycles were not evaluated.

## Data availability

The authors confirm that the data supporting the finding of this study are available within the article. Additional information can be provided from the corresponding author upon request.

## Conflicts of interest

The authors report that there are no competing interest to declare.

## Acknowledgements

Inês D. Borges acknowledges the financial support by the Portuguese Fundação para a Ciência e a Tecnologia (FCT) grant PD/BD/153599/2022. This work was partially supported by project “NATURAL – Nano-argilas para remoção/captura de fosfatos (P) e sua reutilização como fertilizante”, with the reference CENTER-01-0247-FEDER-047080, supported by the Centro Portugal Regional Operational Programme (CENTRO 2020), under the Portugal 2020 (P 2020) Partnership Agreement, through the European Regional Development Fund (ERDF). This work was developed within the scope of the project CICECO – Aveiro Institute of Materials, UID/50011/2025 (DOI: [10.54499/UID/50011/2025](https://doi.org/10.54499/UID/50011/2025)) & LA/P/0006/2020 (DOI: [10.54499/LA/P/0006/2020](https://doi.org/10.54499/LA/P/0006/2020)), financed by national funds through the FCT/MCTES (PIDDAC). This work was carried out within the CERES Centre and supported by national funds from FCT through the projects <https://doi.org/10.54499/UID/00102/2025> and <https://doi.org/10.54499/UID/PRR/00102/2025>.

## References

- 1 S. Daneshgar, A. Callegari, A. G. Capodaglio and D. Vaccari, The potential phosphorus crisis: Resource conservation and possible escape technologies: A review, *Resources*, 2018, 7(2), 37, DOI: [10.3390/resources7020037](https://doi.org/10.3390/resources7020037).
- 2 A. Pfitzner, M. F. Bräun, J. Zweck, G. Brunklaus and H. Eckert, Phosphorus nanorods - Two allotropic modifications of a long-known element, *Angew. Chem., Int. Ed.*, 2004, 43(32), 4228–4231, DOI: [10.1002/anie.200460244](https://doi.org/10.1002/anie.200460244).



- 3 L. Xiao, Y. Li, Q. Kong and Y. Lan, From wastes to functions: preparation of layered double hydroxides from industrial waste and its removal performance towards phosphates, *Environ. Sci. Pollut. Res.*, 2022, **29**(8), 11893–11906, DOI: [10.1007/s11356-021-16563-x](https://doi.org/10.1007/s11356-021-16563-x).
- 4 A. F. Santos, A. L. Arim, D. V. Lopes, L. M. Gando-Ferreira and M. J. Quina, Recovery of phosphate from aqueous solutions using calcined eggshell as an eco-friendly adsorbent, *J. Environ. Manage.*, 2019, **238**, 451–459, DOI: [10.1016/j.jenvman.2019.03.015](https://doi.org/10.1016/j.jenvman.2019.03.015).
- 5 B. Cieřlik and P. Konieczka, A review of phosphorus recovery methods at various steps of wastewater treatment and sewage sludge management. The concept of 'no solid waste generation' and analytical methods, *J. Cleaner Prod.*, 2017, **142**, 1728–1740, DOI: [10.1016/j.jclepro.2016.11.116](https://doi.org/10.1016/j.jclepro.2016.11.116).
- 6 Y. V. Nancharaiah, S. Venkata Mohan and P. N. L. Lens, Recent advances in nutrient removal and recovery in biological and bioelectrochemical systems, *Bioresour. Technol.*, 2016, **215**, 173–185, DOI: [10.1016/j.biortech.2016.03.129](https://doi.org/10.1016/j.biortech.2016.03.129).
- 7 H. Yan, Q. Chen, J. Liu, Y. Feng and K. Shih, Phosphorus recovery through adsorption by layered double hydroxide nano-composites and transfer into a struvite-like fertilizer, *Water Res.*, 2018, **145**, 721–730, DOI: [10.1016/j.watres.2018.09.005](https://doi.org/10.1016/j.watres.2018.09.005).
- 8 V. Carrillo, B. Fuentes, G. Gómez and G. Vidal, Characterization and recovery of phosphorus from wastewater by combined technologies, *Rev. Environ. Sci. Biotechnol.*, 2020, **19**(2), 389–418, DOI: [10.1007/s11157-020-09533-1](https://doi.org/10.1007/s11157-020-09533-1).
- 9 Y. Ye, *et al.*, Insight into chemical phosphate recovery from municipal wastewater, *Sci. Total Environ.*, 2017, **576**, 159–171, DOI: [10.1016/j.scitotenv.2016.10.078](https://doi.org/10.1016/j.scitotenv.2016.10.078).
- 10 M. Khitous, Z. Salem and D. Halliche, Removal of phosphate from industrial wastewater using uncalcined MgAl-NO<sub>3</sub> layered double hydroxide: batch study and modeling, *Desalin. Water Treat.*, 2016, **57**(34), 15920–15931, DOI: [10.1080/19443994.2015.1077745](https://doi.org/10.1080/19443994.2015.1077745).
- 11 M. A. Maia, G. L. Dotto, O. W. Perez-Lopez and M. Gutterres, Phosphate removal from industrial wastewaters using layered double hydroxides, *Environ. Technol.*, 2021, **42**(20), 3095–3105, DOI: [10.1080/09593330.2020.1722257](https://doi.org/10.1080/09593330.2020.1722257).
- 12 J. Q. Jiang and S. M. Ashekuzaman, Preparation and evaluation of layered double hydroxides (LDHs) for phosphate removal, *Desalin. Water Treat.*, 2015, **55**(3), 836–843, DOI: [10.1080/19443994.2014.934734](https://doi.org/10.1080/19443994.2014.934734).
- 13 Z. Xu, Y. Zhong, Y. Wang, X. Song and W. Huang, Removal performance and mechanism of phosphorus by different Fe-based layered double hydroxides, *Environ. Sci. Pollut. Res.*, 2022, **29**, 74591–74601, DOI: [10.1007/s11356-022-21047-7](https://doi.org/10.1007/s11356-022-21047-7).
- 14 N. Baliarsingh, K. M. Parida and G. C. Pradhan, Influence of the nature and concentration of precursor metal ions in the brucite layer of LDHs for phosphate adsorption-a review, *RSC Adv.*, 2013, **3**(46), 23865–23878, DOI: [10.1039/c3ra42857e](https://doi.org/10.1039/c3ra42857e).
- 15 S. Y. Lee, J. W. Choi, K. G. Song, K. Choi, Y. J. Lee and K. W. Jung, Adsorption and mechanistic study for phosphate removal by rice husk-derived biochar functionalized with Mg/Al-calcined layered double hydroxides via co-pyrolysis, *Composites, Part B*, 2019, **176**, 107209, DOI: [10.1016/j.compositesb.2019.107209](https://doi.org/10.1016/j.compositesb.2019.107209).
- 16 J. He, M. Wei, B. Li, Y. Kang, D. Evans G, and X. Duan, Preparation of Layered Double Hydroxides, in *Layered Double Hydroxide*, ed. X. Duan and D. G. Evans, Springer, Berlin Heidelberg, 1st edn, 2006, vol. 119, pp. 90–115, DOI: [10.1016/B978-0-08-098258-8.00025-0](https://doi.org/10.1016/B978-0-08-098258-8.00025-0).
- 17 S. Jamil, A. R. Alvi, S. R. Khan and M. R. S. A. Janjua, Layered Double Hydroxides(LDHs): Synthesis & Applications, *Prog. Chem.*, 2019, **31**(2–3), 394–412, DOI: [10.7536/PC180505](https://doi.org/10.7536/PC180505).
- 18 P. S. Jijoe, S. R. Yashas and H. P. Shivaraju, Fundamentals, synthesis, characterization and environmental applications of layered double hydroxides: a review, *Environ. Chem. Lett.*, 2021, **19**(3), 2643–2661, DOI: [10.1007/s10311-021-01200-3](https://doi.org/10.1007/s10311-021-01200-3).
- 19 S. P. Newman and W. Jones, Synthesis, characterization and applications of layered double hydroxides containing organic guests, *New J. Chem.*, 1998, **22**(2), 105–115, DOI: [10.1039/a708319j](https://doi.org/10.1039/a708319j).
- 20 X. Wang, *et al.*, Efficient removal and selective recovery of phosphorus by calcined La-doped layered double hydroxides, *J. Water Process Eng.*, 2022, **47**(February), 102722, DOI: [10.1016/j.jwpe.2022.102722](https://doi.org/10.1016/j.jwpe.2022.102722).
- 21 S. M. Ashekuzzaman and J. Q. Jiang, Strategic phosphate removal/recovery by a re-usable Mg-Fe-Cl layered double hydroxide, *Process Saf. Environ. Prot.*, 2017, **107**, 454–462, DOI: [10.1016/j.psep.2017.03.009](https://doi.org/10.1016/j.psep.2017.03.009).
- 22 K. Yang, *et al.*, Adsorptive removal of phosphate by Mg-Al and Zn-Al layered double hydroxides: Kinetics, isotherms and mechanisms, *Sep. Purif. Technol.*, 2014, **124**, 36–42, DOI: [10.1016/j.seppur.2013.12.042](https://doi.org/10.1016/j.seppur.2013.12.042).
- 23 C. Novillo, D. Guaya, A. Allen-Perkins Avendaño, C. Armijos, J. L. Cortina and I. Cota, Evaluation of phosphate removal capacity of Mg/Al layered double hydroxides from aqueous solutions, *Fuel*, 2014, **138**, 72–79, DOI: [10.1016/j.fuel.2014.07.010](https://doi.org/10.1016/j.fuel.2014.07.010).
- 24 J. Zhou, S. Yang, J. Yu and Z. Shu, Novel hollow microspheres of hierarchical zinc-aluminum layered double hydroxides and their enhanced adsorption capacity for phosphate in water, *J. Hazard. Mater.*, 2011, **192**(3), 1114–1121, DOI: [10.1016/j.jhazmat.2011.06.013](https://doi.org/10.1016/j.jhazmat.2011.06.013).
- 25 J. T. Klopogee and R. L. Frost, Infrared and Raman Spectroscopic Studies of Layered Double Hydroxides (LDHs), in *Layered Double Hydroxides: Present and Future*, ed. V. Rives, Nova Science Publishers Inc., New York, 1st edn, 2001, pp. 128–153.
- 26 E. Alibakhshi, E. Ghasemi, M. Mahdavian and B. Ramezanzadeh, Corrosion inhibitor release from Zn-Al-[PO<sub>4</sub>]-[CO<sub>3</sub>] layered double hydroxide nanoparticles, *Prog. Color. Coat.*, 2016, **9**(4), 233–248.
- 27 H. Asghar, V. Maurino and M. A. Iqbal, Development of Highly Photoactive Mixed Metal Oxide (MMO) Based on



- the Thermal Decomposition of ZnAl-NO<sub>3</sub>-LDH, *Eng*, 2024, 5(2), 589–599, DOI: [10.3390/eng5020033](https://doi.org/10.3390/eng5020033).
- 28 R. Sasai, *et al.*, Why Do Carbonate Anions Have Extremely High Stability in the Interlayer Space of Layered Double Hydroxides? Case Study of Layered Double Hyd Consisting of Mg and Al (Mg/Al = 2), *Inorg. Chem.*, 2019, 58(16), 10928–10935, DOI: [10.1021/acs.inorgchem.9b01365](https://doi.org/10.1021/acs.inorgchem.9b01365).
  - 29 X. Chen, X. Cheng, D. Sun, W. Ma and X. Wang, Adsorptive removal of phosphate from secondary effluents in WWTPs by ZnAl layered double hydroxides granules, *Desalin. Water Treat.*, 2015, 54(4–5), 1216–1225, DOI: [10.1080/19443994.2014.950338](https://doi.org/10.1080/19443994.2014.950338).
  - 30 Y. Jia, *et al.*, Kinetics, isotherms and multiple mechanisms of the removal for phosphate by Cl-hydrocalumite, *Appl. Clay Sci.*, 2016, 129, 116–121, DOI: [10.1016/j.clay.2016.05.018](https://doi.org/10.1016/j.clay.2016.05.018).
  - 31 Y. H. Jiang, A. Y. Li, H. Deng, C. H. Ye and Y. Li, Phosphate adsorption from wastewater using ZnAl-LDO-loaded modified banana straw biochar, *Environ. Sci. Pollut. Res.*, 2019, 26(18), 18343–18353, DOI: [10.1007/s11356-019-05183-1](https://doi.org/10.1007/s11356-019-05183-1).
  - 32 EPA, Method 365.3: Phosphorus, All Forms (Colorimetric, Ascorbic Acid, Two Reagent), 1978, online, available: [https://www.epa.gov/sites/default/files/2015-08/documents/method\\_365-3\\_1978.pdf](https://www.epa.gov/sites/default/files/2015-08/documents/method_365-3_1978.pdf).
  - 33 E. M. Seftel, R. G. Ciocarlan, B. Michielsen, V. Meynen, S. Mullens and P. Cool, Insights into phosphate adsorption behavior on structurally modified ZnAl layered double hydroxides, *Appl. Clay Sci.*, 2018, 165, 234–246, DOI: [10.1016/j.clay.2018.08.018](https://doi.org/10.1016/j.clay.2018.08.018).
  - 34 S. Bin Lee, E. H. Ko, J. Y. Park and J. M. Oh, Mixed metal oxide by calcination of layered double hydroxide: Parameters affecting specific surface area, *Nanomaterials*, 2021, 11(5), 1–19, DOI: [10.3390/nano11051153](https://doi.org/10.3390/nano11051153).
  - 35 G. Mishra, B. Dash and S. Pandey, Layered double hydroxides: A brief review from fundamentals to application as evolving biomaterials, *Appl. Clay Sci.*, 2018, 153, 172–186, DOI: [10.1016/j.clay.2017.12.021](https://doi.org/10.1016/j.clay.2017.12.021).
  - 36 W. Liao, X. P. Liu, H. Q. Li and P. Yang, Simultaneous removal of phosphate and nitrate on calcined Mg-Al layered double hydroxides, *Pol. J. Environ. Stud.*, 2020, 29(1), 187–195, DOI: [10.15244/pjoes/94991](https://doi.org/10.15244/pjoes/94991).
  - 37 R. Chitrakar, S. Tezuka, A. Sonoda, K. Sakane, K. Ooi and T. Hirotsu, Adsorption of phosphate from seawater on calcined MgMn-layered double hydroxides, *J. Colloid Interface Sci.*, 2005, 290(1), 45–51, DOI: [10.1016/j.jcis.2005.04.025](https://doi.org/10.1016/j.jcis.2005.04.025).
  - 38 P. Cai, *et al.*, Competitive adsorption characteristics of fluoride and phosphate on calcined Mg-Al-CO<sub>3</sub> layered double hydroxide, *J. Hazard. Mater.*, 2012, 100–108, DOI: [10.1016/j.jhazmat.2012.01.069](https://doi.org/10.1016/j.jhazmat.2012.01.069).
  - 39 J. Buates and T. Imai, Biochar functionalization with layered double hydroxides composites: Preparation, characterization, and application for effective phosphate removal, *J. Water Process Eng.*, 2020, 37, 101508, DOI: [10.1016/j.jwpe.2020.101508](https://doi.org/10.1016/j.jwpe.2020.101508).
  - 40 A. K. A. Khalil, F. Dweiri, I. W. Almanassra, A. Chatla and M. A. Atieh, Mg-Al Layered Double Hydroxide Doped Activated Carbon Composites for Phosphate Removal from Synthetic Water: Adsorption and Thermodynamics Studies, *Sustainability*, 2022, 14(12), 6991, DOI: [10.3390/su14126991](https://doi.org/10.3390/su14126991).
  - 41 Q. Zhang, *et al.*, Systematic screening of layered double hydroxides for phosphate removal and mechanism insight, *Appl. Clay Sci.*, 2019, 174, 159–169, DOI: [10.1016/j.clay.2019.03.030](https://doi.org/10.1016/j.clay.2019.03.030).
  - 42 J. W. Son, *et al.*, Analysis of phosphate removal from aqueous solutions by hydrocalumite, *Desalin. Water Treat.*, 2016, 57(45), 21476–21486, DOI: [10.1080/19443994.2015.1119759](https://doi.org/10.1080/19443994.2015.1119759).
  - 43 K. L. Tan and B. H. Hameed, Insight into the adsorption kinetics models for the removal of contaminants from aqueous solutions, *J. Taiwan Inst. Chem. Eng.*, 2017, 74, 25–48, DOI: [10.1016/j.jtice.2017.01.024](https://doi.org/10.1016/j.jtice.2017.01.024).
  - 44 J. Das, B. S. Patra, N. Baliarsingh and K. M. Parida, Adsorption of phosphate by layered double hydroxides in aqueous solutions, *Appl. Clay Sci.*, 2006, 32(3–4), 252–260, DOI: [10.1016/j.clay.2006.02.005](https://doi.org/10.1016/j.clay.2006.02.005).
  - 45 T. Sudare, A. Zenzai, S. Tamura, M. Kiyama, F. Hayashi and K. Teshima, Hierarchical spheres of Mg-Al LDH for the removal of phosphate ions: Effect of alumina polymorph as precursor, *CrystEngComm*, 2019, 21(47), 7211–7216, DOI: [10.1039/c9ce01064e](https://doi.org/10.1039/c9ce01064e).
  - 46 B. Kostura, D. Matýšek, J. Kukutschová and J. Leško, Phosphate interaction with calcined form of Mg-Al-CO<sub>3</sub> hydrotalcite in aqueous solutions, *Ann. Chim.: Sci. Mater.*, 2012, 37(1), 11–20, DOI: [10.3166/acsm.37.11-20](https://doi.org/10.3166/acsm.37.11-20).
  - 47 C. Gomes, M. Zahid, R. Sampaio, A. Bastos, J. Tedim, M. Frederico, R. Cláudia and F. Mario, Use of ZnAl-Layered Double Hydroxide (LDH) to extend the service life of reinforced concrete, *Materials*, 2020, 13(7), 1769, DOI: [10.3390/MA13071769](https://doi.org/10.3390/MA13071769).
  - 48 G. Zhang, *et al.*, Active corrosion protection by a smart coating based on a MgAl-layered double hydroxide on a cerium-modified plasma electrolytic oxidation coating on Mg alloy AZ31, *Corros. Sci.*, 2018, 139(January), 370–382, DOI: [10.1016/j.corsci.2018.05.010](https://doi.org/10.1016/j.corsci.2018.05.010).
  - 49 F. Hu, *et al.*, High-efficient adsorption of phosphates from water by hierarchical CuAl/biomass carbon fiber layered double hydroxide, *Colloids Surf., A*, 2018, 555, 314–323, DOI: [10.1016/j.colsurfa.2018.07.010](https://doi.org/10.1016/j.colsurfa.2018.07.010).

